

Comparative Analysis of High Resolution Gridded Satellite Precipitation Products over Ganga Basin in India

Singla S.^{1*}, Rachit¹, Thakur P.K.¹ and Garg V.¹

¹Water Resources Department, Indian Institute of Remote Sensing, Indian Space Research Organisation, Dehradun, India

[*sanyamsingla0504@gmail.com](mailto:sanyamsingla0504@gmail.com)

Abstract: *The High resolution precipitation datasets play a significant role in hydrological simulations and water resource management. The varying topography and uneven distribution of rain gauge stations in Ganga basin emphasis on utilizing the Satellite Precipitation products. In this study, the performances of Integrated Multi-Satellite Retrieval for GPM (IMERG) Version 07 and the Global Satellite Mapping of Precipitation (GSMaP) developed by ISRO and JAXA at $0.1 \times 0.1^\circ$ gridded scale were compared with Indian Meteorological Department (IMD) ground based $0.25 \times 0.25^\circ$ gridded data from year 2001-2023 as per the availability of datasets. The analysis was performed using continuous evaluation metrics (Relative Bias (RBias), Relative Root Mean Square Error (RRMSE), Relative Mean Absolute Error (RMAE), Pearson's Correlation coefficient (Rp)) and categorical metrics (Probability of Detection (POD), False Alarm Ratio (FAR), Critical Success index (CSI), Frequency Bias Index (FBI)) for monsoon season and for rainfall (mm) events (No Rain (0), Light Rain (0.1-7.5), Moderate Rain (7.6-64.4), Heavy Rain (64.5-124.4), Very Heavy Rain (124.5 or more)) defined by IMD based on rainfall intensities. The results showed an increase in RBias in mountainous regions having high altitude whereas lower values of POD in these regions. The IMERG and GSMaP were found to be fairly comparable with CC values of IMERG ranging from (-0.05 to 0.65) and GSMaP ranging from (-0.15 to 0.75). In case of No Rain and Light Rain events, the IMERG and GSMaP showed good detection capabilities, however with the increase in intensities of rainfall events, the values of POD decreased and the values of FAR increased. The above results suggest that though satellite precipitation products cannot be an alternative to ground-based observations but reliable datasets for low intensity precipitation studies and for filling the gaps where there is no data availability.*

Keywords: Precipitation, Ganga Basin, IMERG, GSMaP, IMD

Introduction

For a country like India, with varying topography ranging from high altitude Himalayan mountains in the North, Indo-Gangetic plains, Thar Desert, Deccan plateau, Eastern and Western Ghats and finally the Indian coastal region, a dynamic phenomenon like precipitation becomes one of the most decisive parameters for assessing water resource management, hydro-climatological, agriculture, disaster and climate change studies. The Ganga basin being the largest river basin of India receives precipitation in a span of nearly 9 lakhs kilometer square land spanning from upper Himalayas to plains in the southern region. Precipitation being a dynamic phenomenon and essential component of the water cycle varying in shape and intensity, its temporal and spatial changes affect regional climatic characteristics (Jeniffer et al., 2010; Ghajarnia et al., 2015). The challenges in the

acquisition of hydro-meteorological data varies like distribution and density of weather stations, inaccuracy or errors in instrument, uncertainties in measurement. Apart from this, overcoming the limitation of unavailability of continuous data over a large region study is partially resolved by satellite-based precipitation products at different spatial and temporal scales (Sharifi et al., 2016). It becomes imperative to determine the accuracies and required corrections for the satellite-based products as they are often accompanied with uncertainties and inherent errors, which might be due to topographical or climate features of the region (AghaKouchak et al., 2009).

Many studies have proposed various satellite-based models for estimation of precipitation e.g. Precipitation Estimation from Remotely Sensed Information using Artificial Neural Networks - Cloud Classification System estimation (PERSIANN-CCS) (Hong et al., 2004), the Climate Hazards group Infrared Precipitation with Stations (CHIRPS) (Funk et al., 2015), the National Oceanic and Atmospheric Administration (NOAA) Climate Prediction Center (CPC) Morphing technique product (CMORPH) (Joyce et al., 2004) and the Tropical Precipitation Measuring Mission (TRMM) Multi-satellite Precipitation Analysis (TMPA) (Huffman et al., 2007).

Literature Review

Dehaghani et al., (2023) critically evaluated three satellite precipitation products that are PERSIANN-CCS, TRMM-3B42RT V7, and CMORPH, across 52 synoptic stations in Iran. They employed metrics like Pearson's correlation coefficient and Relative Root Mean Square Error to assess accuracy. As key highlights, PERSIANN-CCS overestimates precipitation but excels in event detection, while TRMM and CMORPH show significant underestimations. The study highlights the importance of bias correction methods, which significantly enhance satellite performance in precipitation estimation.

In another study, carried out by Zhu et al., (2022), they evaluated the performance of satellite precipitation products, IMERG and GSMaP, against rain gauge observations in Northern China. They highlighted the limitations posed by uneven rain gauge distribution and complex topography, which affect the accuracy of satellite estimates. The study finds that GSMaP performs better in non-typhoon events, while IMERG excels during typhoons. The specific evaluation metrics used include Correlation Coefficient (CC), Relative Bias (RB),

Root Mean Square Error (RMSE), Fraction Skill Score (FSE), Probability of Detection (POD), False Alarm Ratio (FAR) and Critical Success Index (CSI).

Rachdane et al., (2022) evaluated six high-resolution satellite precipitation products in sub-Saharan Morocco from 2000 to 2020, to address the sparse gauge network issue. They used similar continuous metrics like Correlation Coefficient, Relative Bias, Relative Root Mean Square Error, Relative Mean Absolute Error and categorical statistical indices, Probability of Detection, False Alarm Ratio and Critical Success Index. at daily, monthly, and annual scales, across pixel and basin levels. GPM-F product performed best overall, while CHIRPS and CCS-CDR were effective at monthly and annual scales, highlighting the varying performance across different altitudes. Tesfaye et al., (2017) in their study found that ERA-Interim and CFSR perform best in replicating rainfall characteristics, while NCEP-DOE R2 tends to overestimate precipitation in Ethiopia. The analysis reveals that observed rainfall shows a higher frequency of short wet spells compared to reanalysis datasets. Additionally, the lack of sufficient observed data limits the accuracy of reanalysis products, highlighting the need for improved data availability.

Study Area

The Ganga basin spans over India, Tibet, Nepal, and Bangladesh covering a total area of 10,86,000 square kilometres. For this study, Ganga basin which is largest basin in India with drainage area of 8,61,452 square kilometres covering the states of Uttarakhand, Himachal Pradesh, Uttar Pradesh, Haryana, Rajasthan, Madhya Pradesh, Bihar, Jharkhand, West Bengal and Chhattisgarh is chosen as shown in (Figure 1). The Ganga basin is extended between north latitudes $21^{\circ}6'$ to $31^{\circ}21'$ and east longitudes $73^{\circ}2'$ to $89^{\circ}5'$ with a maximum width of 1024 km and length of 1543km. With a diverse topography, Ganga Basin is dominated by mountains in the North with Mount Everest reaching up to a height of 8848 metres above mean sea level whereas the middle basin is predominated by flat plains within 100 meters above mean sea level and a delta in the basin's southeast at 5m above mean sea level is home to the vast Sundarbans mangrove systems.

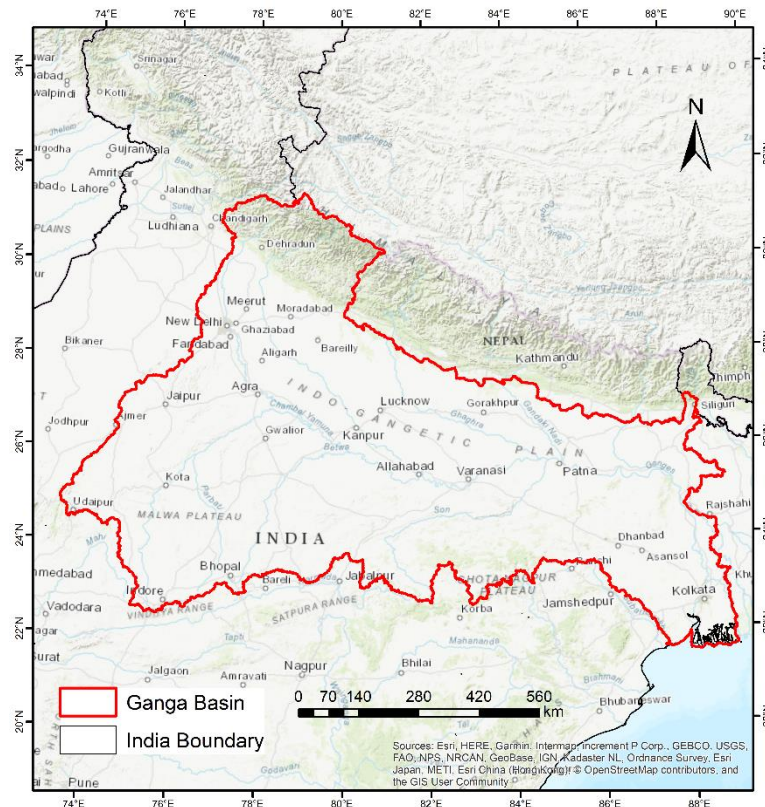


Figure 1: Study area map

Datasets

a. IMD gridded dataset as observation data

The observation dataset is daily interpolated observations from 6995 rain gauge stations, all over India, obtained from the India Meteorological Department (IMD) (Pai et al., 2014). The time period of the dataset used was 2001 to 2023. The downloaded data was clipped according to Ganga basin boundary. The spatial resolution of the grid values is $0.25^\circ \times 0.25^\circ$, which is nearly 27830 meters. This gridded dataset was prepared after carrying out quality control of basic rain-gauge stations.

b. Satellite-derived precipitation dataset

The Integrated Multi-Satellite Retrievals for the Global Precipitation Measurement (IMERG) version 7 provided by NASA which combines multiple satellite data (primarily Global Precipitation Measurement (GPM) mission) to create accurate precipitation estimates for land as well as the ocean. It is a high-resolution dataset providing near-real-time precipitation data with a temporal resolution of 30 minutes and spatial resolution of approximately 0.1 degrees (about 10 km). It finds its usefulness in various hydro-climatological research studies, weather forecasting and hydrological modeling.

The other recently made available precipitation dataset Global Satellite Mapping of Precipitation (GSMaP) developed by the Indian Space Research Organisation (ISRO) and Japan Aerospace Exploration Agency (JAXA) through Implementation of Agreement (IA) specially for the Indian subcontinent (Kumar et al., 2024), is used for performance evaluation. It is available from March 2000 onwards with spatial resolution of $0.1^\circ \times 0.1^\circ$ and a temporal resolution of 1 hour. This product integrates India Meteorological Department (IMD) gauge correction apart from being based on the GSMaP algorithm (Kubota et al. 2020; Kumar et al. 2021, 2022). The JAXA created the GSMaP algorithm that plays a critical role in providing a complete picture of precipitation based on microwave radiometer data and cloud motion from Geostationary Infrared (IR). These are the three main categories through which the algorithm is split up to measure it properly: microwave imager, microwave sounder, and a combination of both microwave-infrared (MVK) as well (Mega et al. 2018).

Methodology

The performance of IMERG and ISRO GSMaP datasets were evaluated with IMD gridded dataset as a reference for monsoon months (June, July, August, September) from year 2001-2023 over Ganga Basin. As there is a spatial and temporal variability in the datasets, the IMD dataset was interpolated to a common resolution $0.1^\circ \times 0.1^\circ$. The accuracy of the satellite datasets was evaluated using continuous and categorical evaluation metrics. The continuous metrics (RRMSE, RMAE, RBias, CC) were computed as shown in Table 1. The CC indicates the spatial and temporal correlation between the datasets, RBias shows systematic biases between the datasets, RRMSE and RMAE represents average error between the datasets.

Table 1: Continuous Evaluation Metrics used in the study.

Metric Name	Equation	Range	Perfect Value
Relative Root mean Square Error (RMSE)	$\sqrt{\frac{\frac{1}{n} \sum_{i=1}^n (S_i - O_i)^2}{\frac{1}{n} \sum_{i=1}^n (O_i)^2}}$	0 to $+\infty$	0
Relative Mean Absolute Error (RMAE)	$\frac{\sum_{i=1}^n S_i - O_i }{\sum_{i=1}^n O_i}$	0 to $+\infty$	0
Relative Bias (RBias)	$\frac{\sum_{i=1}^n (S_i - O_i)}{\sum_{i=1}^n O_i} * 100$	0 to $+\infty$	0
Pearson's Correlation Coefficient (CC)	$\frac{\sum_{i=1}^n (O_i - \bar{O})(S_i - \bar{S})}{\sqrt{\sum_{i=1}^n (O_i - \bar{O})^2} * \sqrt{\sum_{i=1}^n (S_i - \bar{S})^2}}$	-1 to +1	1

The satellite datasets and reference dataset were categorized based on the five rainfall intensities events (No Rain, Light Rain, Moderate Rain, Heavy Rain, very heavy Rain) defined by IMD as shown in Table 2.

Table 2: Categorization of precipitation events.

Rainfall Event	Intensity (mm/day)
No Rain	0
Light Rain	0.1-7.5
Moderate Rain	7.6-35.5
Heavy Rain	64.5-124.4
Very heavy Rain	≥ 124.5

The contingency matrix was developed (as shown in Table 3) for computing categorical evaluation metrics (POD, FAR, CSI, FBI) as shown in Table 4. The skill of satellite precipitation products in detecting real precipitation events is expressed by the Probability of Detection (POD). The False Alarm Ratio (FAR) measures the extent of false detections in IMERG and GSMaP precipitation estimates. The Critical Success Index (CSI) is another quality measure that considers both POD and FAR, offering a comprehensive evaluation of the capacity of satellite-based Quantitative Precipitation Estimates (QPE) to detect actual precipitation events as a whole.

Table 3: Categorization of satellite rainfall intensities events.

	Observations exceeds a threshold level	Yes	No
Satellite Data exceeds a threshold level	Yes	Hits	False Alarms
	No	Misses	Correct Negatives

Table 4: Categorical Evaluation Metrics used in the study.

Categorical Evaluation Metrics	Equation	Range	Perfect Value
Probability of Detection (POD)	$\frac{\text{Hits}}{\text{Hits} + \text{Misses}}$	0 to 1	1
False Alarm Ratio (FAR)	$\frac{\text{False Alarms}}{\text{Hits} + \text{False Alarms}}$	0 to 1	0
Critical Success Index (CSI)	$\frac{\text{Hits}}{\text{Hits} + \text{Misses} + \text{False Alarms}}$	0 to 1	1
Frequency Bias Index	$\frac{\text{Hits} + \text{False Alarms}}{\text{Hits} + \text{Misses}}$	0 to $+\infty$	1

Results

The comparative analysis of the IMERG and GSMaP precipitation products against IMD rainfall data over the Ganga Basin, especially focusing on the scale of important evaluation metrics as those definitely capture their power to duplicate rainfall patterns. The specific scales for mean seasonal maps, Relative Bias (RBias), Relative Root Mean Square Error (RRMSE), Relative Mean Absolute Error (RMAE), and Pearson's Correlation Coefficient (Rp) provided in this study further enrich the perspective on whether these satellite precipitation products are skillful or not.

a. Average Seasonal Rainfall (JJAS) from 2001–2023

The key differences in the spatial distribution of mean seasonal rainfall, which ranges from 0 to 3000 mm, are evident between GSMaP, IMERG, and IMD as shown in (Figure 2,3,4). GSMaP, with average values from 500 mm to 1500 mm, shows improved performance in representing rainfall distribution, particularly in the northern mountainous areas where rainfall peaks around 2500–3000 mm. IMERG, however, frequently shows rainfall exceeding 2500 mm in the northern regions, which is an overestimation compared to GSMaP's slight overestimation.

In the southern plains, IMERG significantly underestimates rainfall (300–600 mm) while substantially overestimating rainfall in the northern high-altitude regions, exceeding 3000 mm. Despite capturing the general monsoon season trends, IMERG shows poor agreement with local rainfall distribution compared to GSMaP.

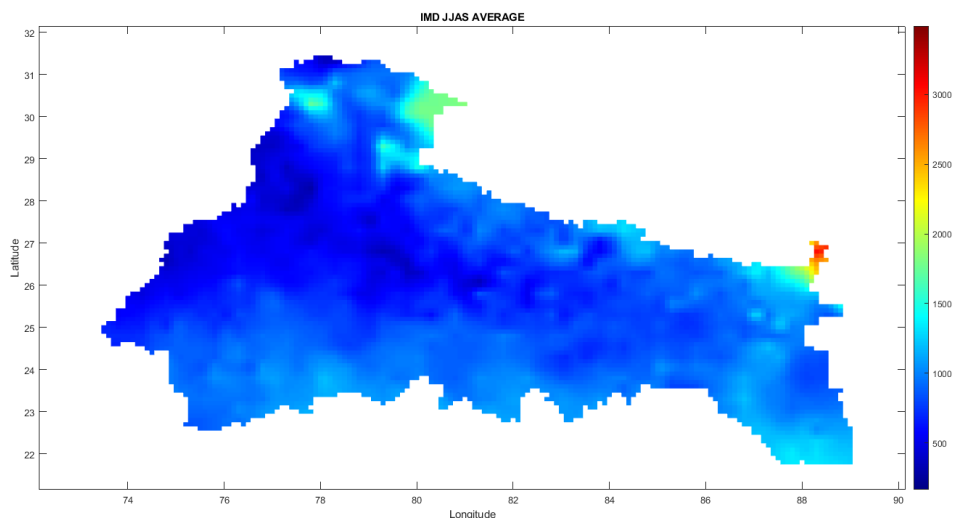


Figure 2: IMD JJAS Average

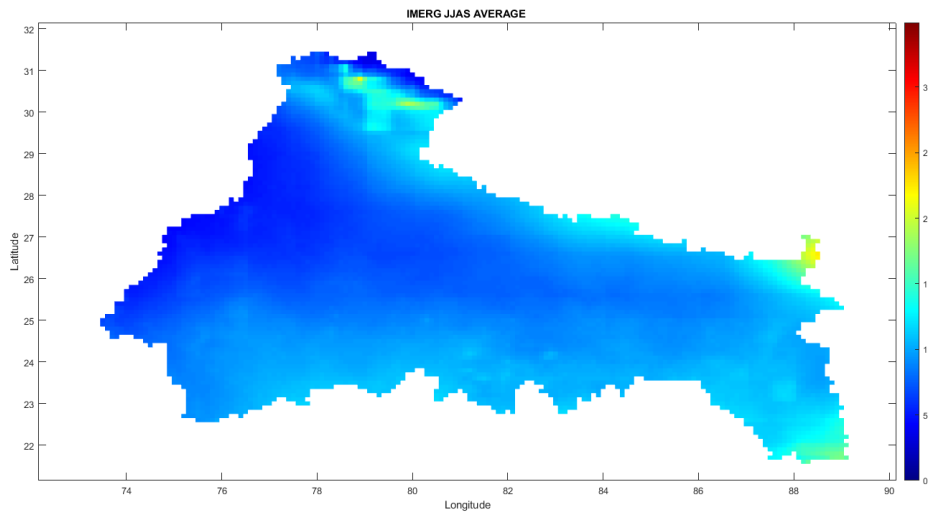


Figure 3: IMERG JJAS Average

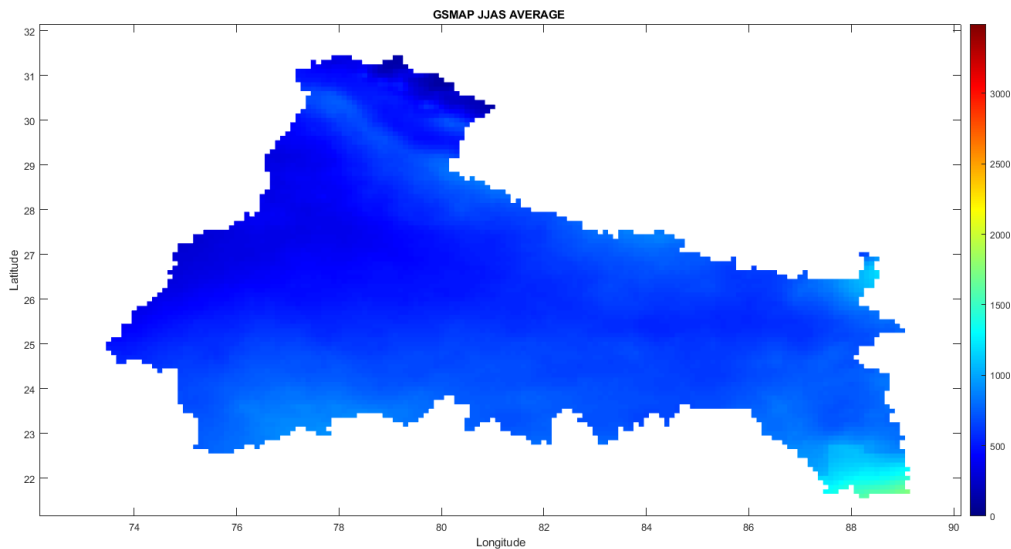


Figure 4: GSMaP JJAS Average

b. Relative Bias (RBias)

It can be observed that RBias values are extremely low, indicating that GSMaP far outperforms in the plains, with RBias values around 0–20, reflecting minimal bias in estimating rainfall as shown in (Figure 6). In high-altitude regions, GSMaP slightly overestimates rainfall, with bias values sometimes reaching 60. However, this remains low compared to IMERG, where RBias values frequently exceed 80 in the mountainous regions, suggesting significant rainfall overestimation as shown in (Figure 5).

In the southern plains, GSMaP shows RBias around 20–30, while IMERG represents rainfall with RBias values approaching 30-40 . This discrepancy suggests that GSMaP handles the basin's topographical variability more effectively, while IMERG faces significant challenges, especially in mountainous and southern plain areas.

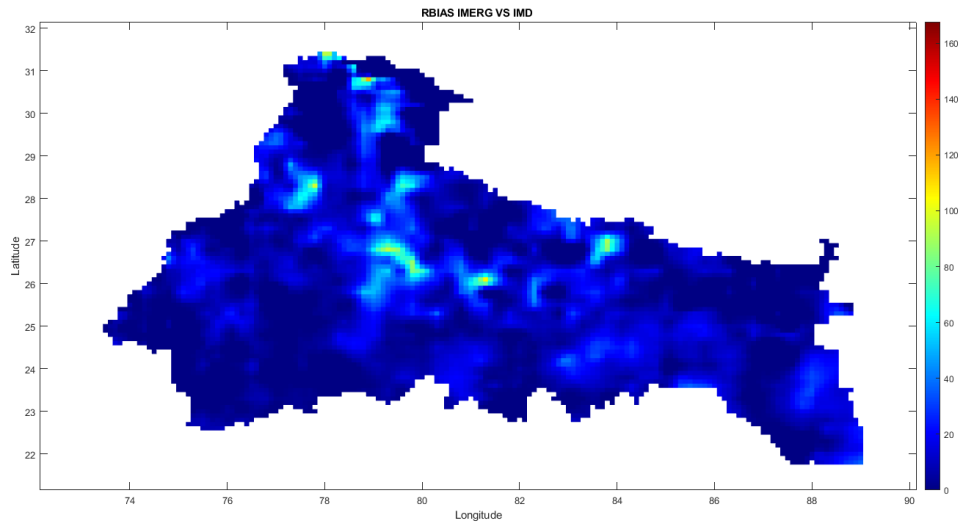


Figure 5: Relative Bias (IMERG vs IMD)

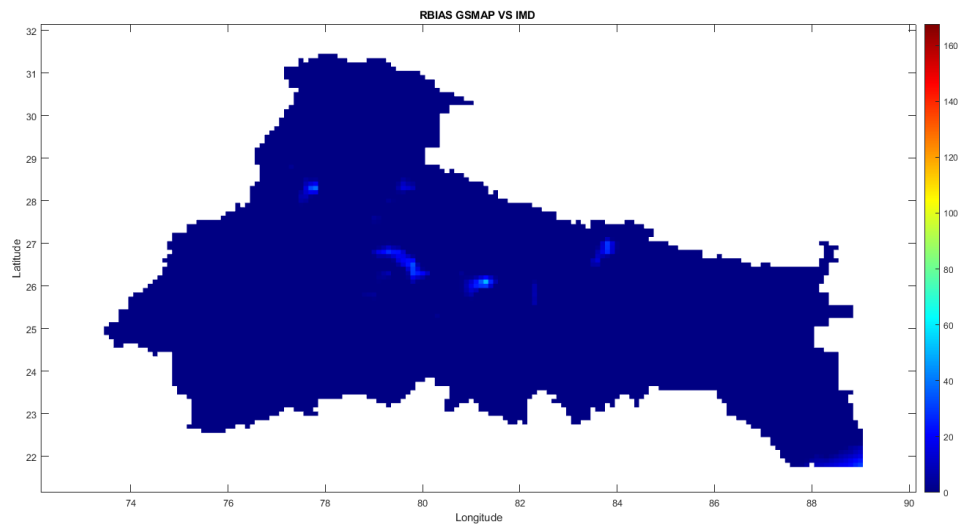


Figure 6: Relative Bias (GSMAP vs IMD)

Relative Root Mean Square Error (RRMSE)

The RRMSE values (in the axis from 0 to 6) as shown in (Figure 7,8) show that GSMaP performs better than IMERG in most cases. The RRMSE for GSMaP, in the plains, is relatively low (0.5–2), indicating a good agreement with IMD data. In the mountainous north, where topography introduces higher magnitude errors, GSMaP is typically accurate to around 3–4 RRMSE. IMERG values are quite high in these regions, often greater than 4, indicating significant departures from observed rainfall patterns. The smallest RRMSE (Root Mean Squared Error) values correspond to GSMaP over the basin, inferring GSMaP's superiority in estimating rainfall in complex terrains, while IMERG's performance is inadequate in critical areas where topography plays a crucial role in rainfall distribution.

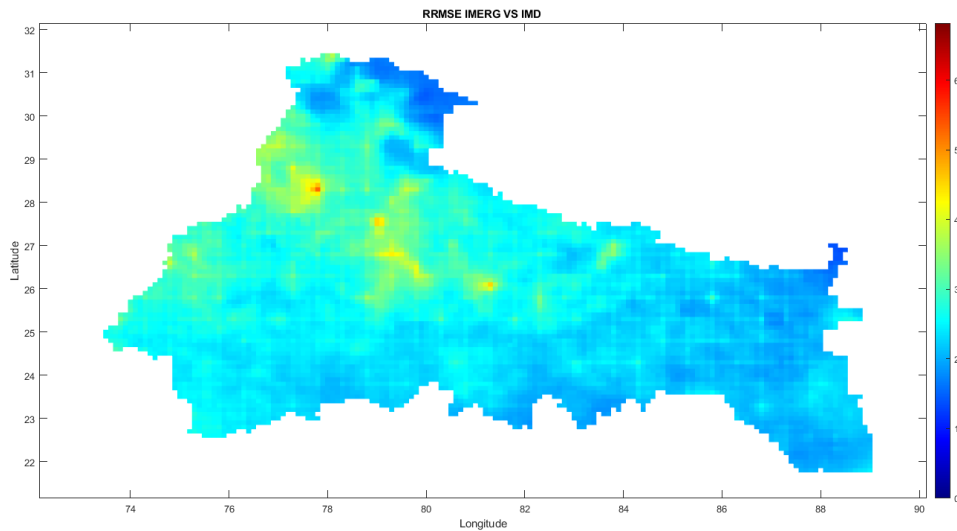


Figure 7: RRMSE (IMERG vs IMD)

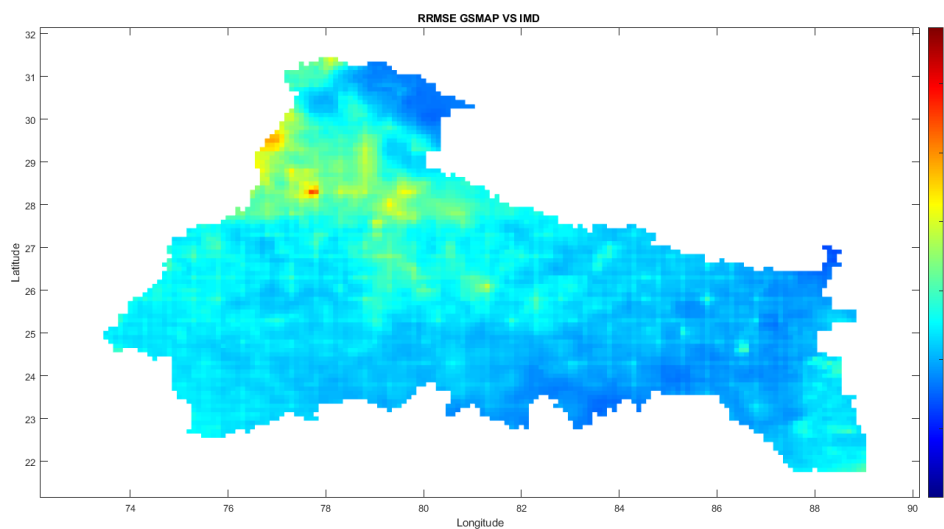


Figure 8: RRMSE (GSMaP vs IMD)

c. Relative Mean Absolute Error (RMAE)

Again, the lower relative error (between 0 and 2) for GSMaP confirms its higher accuracy as shown in (Figure 10). RMAE values between 0.5 and 1 found in the plains correlate with high levels of goodness-of-fit to observed rainfall in case of GSMaP. At higher elevations, the RMAE increases to around 1.5 and remains lower than IMERG's, frequently greater than 1.5 in the north. IMERG's RMAE in the plains is somewhat higher than GSMaP, around 1–1.2 as shown in (Figure 9). The lower RMAE values for GSMaP support its robustness in estimating rainfall across broader topographical conditions.

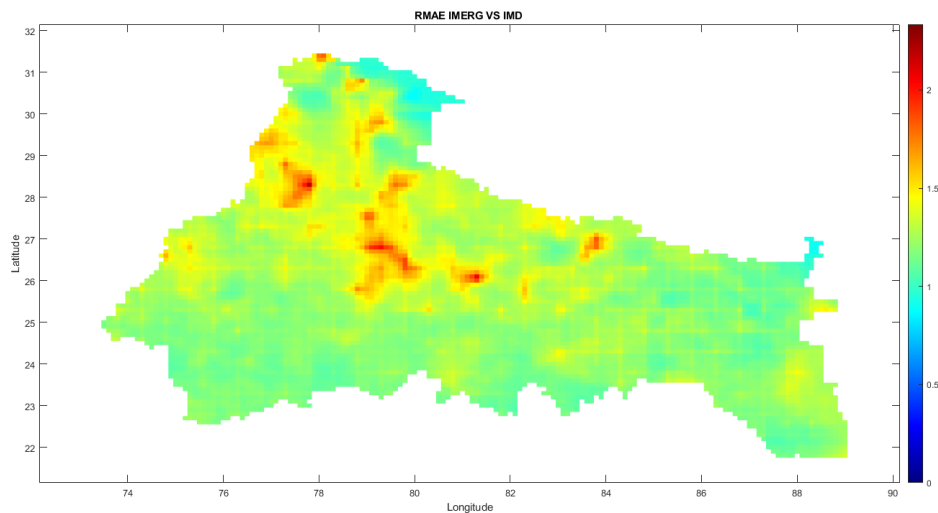


Figure 9: RMAE (IMERG vs IMD)

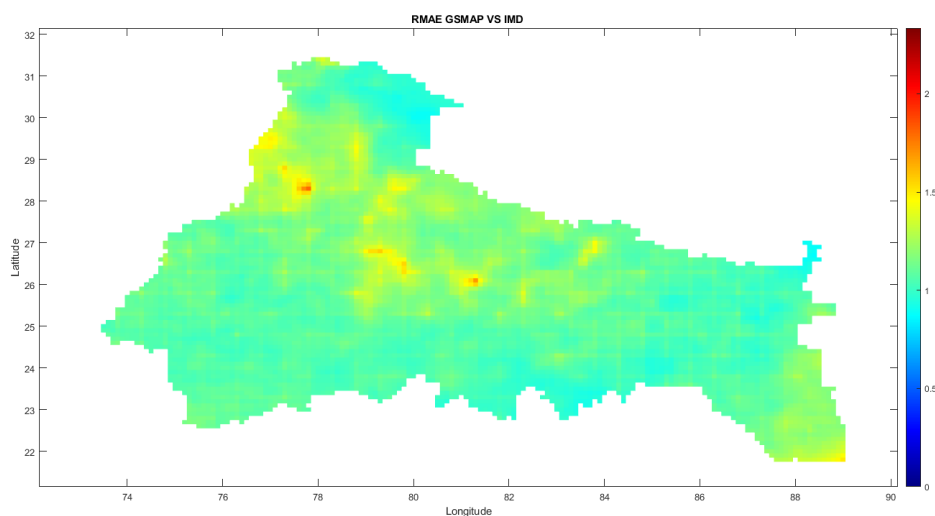


Figure 10: RMAE (GSMaP vs IMD)

d. Pearson's Correlation Coefficient (R_p)

Values of the Pearson's Correlation Coefficient (R_p), with a range of 0–0.45, support GSMaP's better performance than IMERG as shown in (Figure 11,12). Over the plains, GSMaP and IMD observations show high R_p values (0.3–0.4), indicating good alignment with IMD data. In contrast, IMERG's correlation values are lower, typically around 0.2–0.3.

In the northern highlands, where both products face challenges due to complex terrain, GSMaP still outperforms IMERG, with R_p values around 0.25–0.3, while IMERG's values drop to 0.1–0.2. This shows GSMaP's stronger ability to capture spatial rainfall variability, even in mountainous areas.

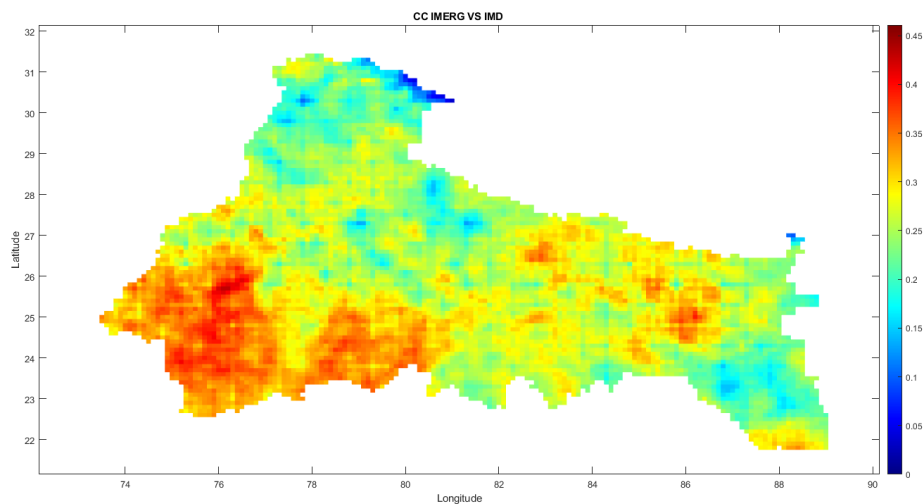


Figure 11: CC (IMERG VS IMD)

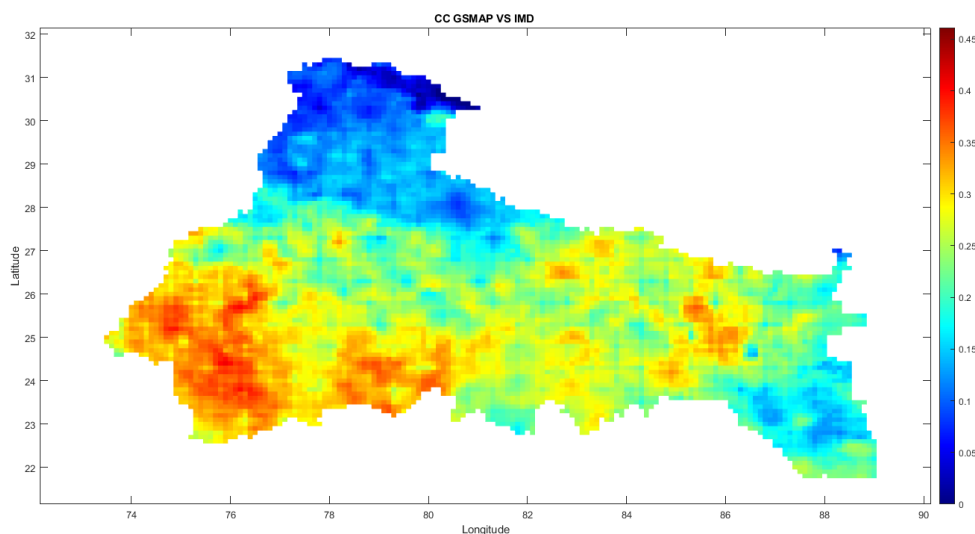


Figure 12: CC (GSMaP VS IMD)

e. Categorical Metrics Analysis

Categorical Metrics Analysis (POD, FAR, CSI, FBI): The categorical metrics analysis, including Probability of Detection (POD), False Alarm Ratio (FAR), Critical Success Index (CSI), and Frequency Bias Index (FBI), provides different insights into the detection capabilities of both products as shown in (Figure 13,14,15,16). For "No Rain" events, GSMaP performs better, with a POD around 0.8, indicating a higher probability of detecting dry conditions. The FAR is low at 0.2, meaning fewer false positives. IMERG's POD for "No Rain" is slightly lower at 0.6, with a FAR of 0.3, reflecting more false detections. For Light and Moderate Rain events, IMERG outperforms GSMaP, with a POD of 0.7–0.8 and CSI around 0.6, indicating superior detection accuracy. GSMaP's POD is lower, at 0.6, and its FAR is higher at 0.4, showing it tends to overestimate these rain events.

The satellite datasets struggle with Heavy and Very Heavy Rain events. GSMaP has a FAR of around 0.5, meaning it overestimates heavy rainfall, and its POD drops to around 0.4. IMERG shows similar behaviour, with a FAR of 0.5 and a POD of 0.3, making both less reliable for extreme rainfall detection. The Frequency Bias Index (FBI) shows GSMaP at about 1.2 for "No Rain" events, indicating a slight overestimation of dry periods. For Light and Moderate Rain, IMERG's FBI is closer to 1, indicating better accuracy, while GSMaP tends to overestimate with an FBI of around 1.3. Both products have FBI values over 1.5 for Heavy and Very Heavy Rain, showing an over-detection trend for extreme rainfall.

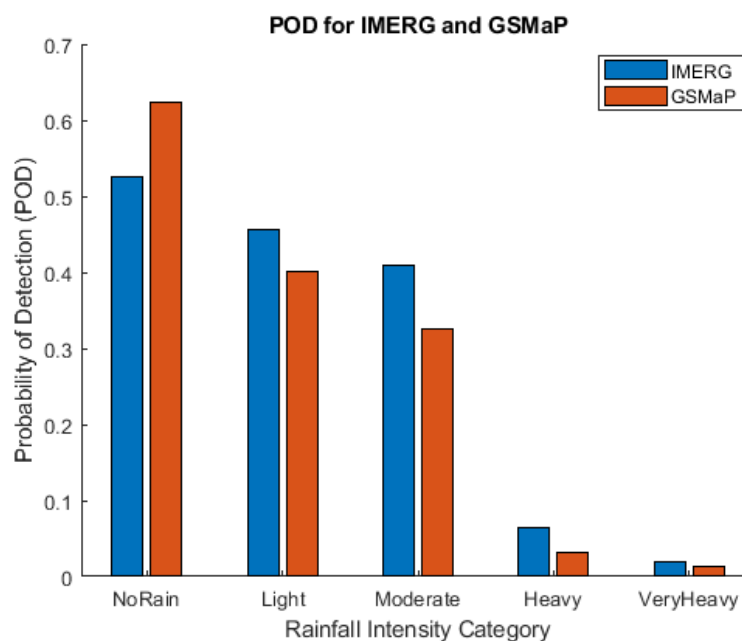


Figure 13: Probability of Detection (POD)

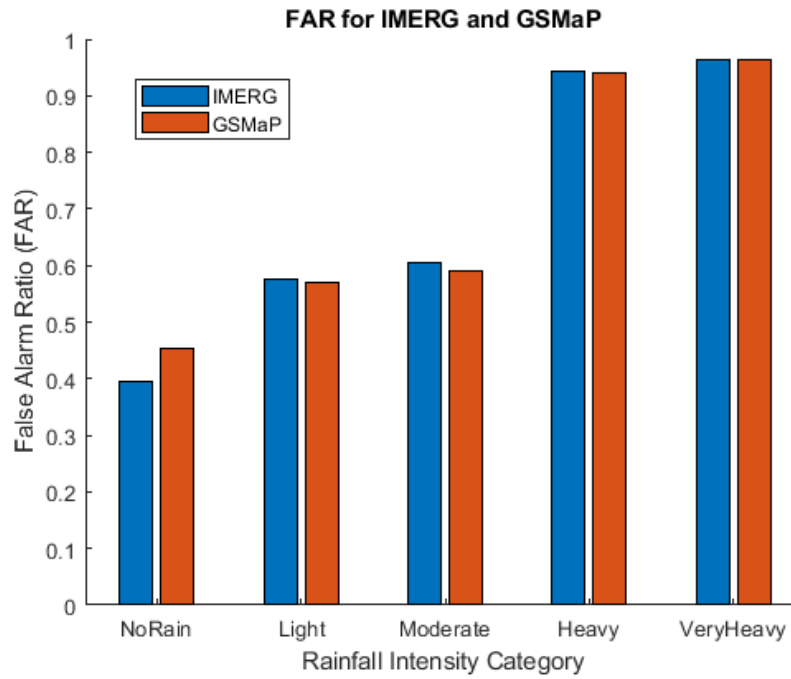


Figure 14: False Alarm ratio (FAR)

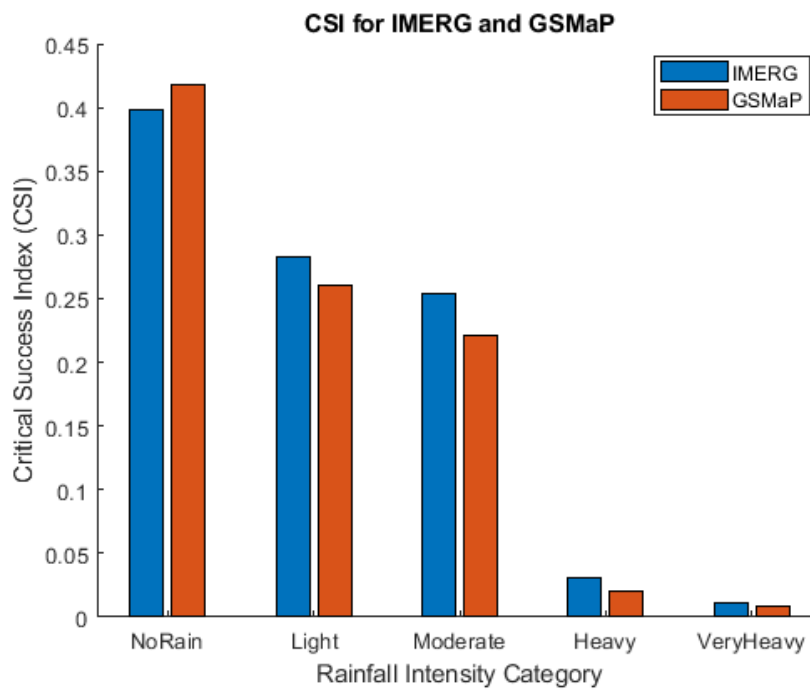


Figure 15: Critical Success Index (CSI)

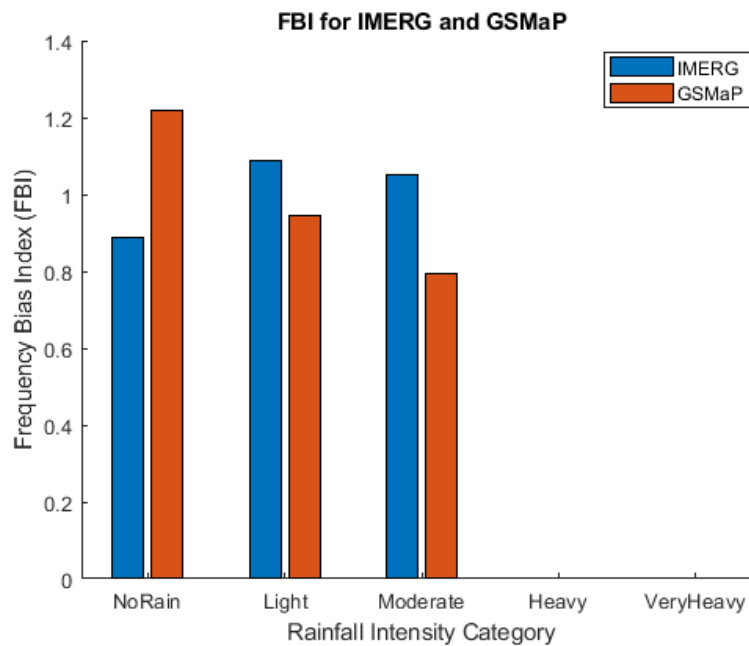


Figure 16: Frequency Bias Index (FBI)

Discussion

The comparison between GSMaP and IMERG highlights GSMaP's consistent performance, particularly over the Ganga Basin's complex terrain and during the monsoon season. Previous studies support the findings that GSMaP is more effective at capturing both spatial and temporal rainfall variability, especially in areas with limited ground-based observations. GSMaP's integration of multiple sensors and real-time gauge calibration improves its accuracy in regions like the northern highlands, where topographical complexity makes rainfall monitoring difficult.

Continuous metrics such as Relative Bias (RBias), Relative Root Mean Square Error (RRMSE), and Relative Mean Absolute Error (RMAE) reveal that GSMaP provides better-calibrated rainfall estimates, particularly in plains and high-altitude regions. In contrast, IMERG demonstrates more significant variability and discrepancies when compared to Indian Meteorological Department (IMD) data, especially in high-altitude areas. The superior calibration and multi-sensor integration of GSMaP help minimize these discrepancies, making it more reliable for rainfall assessments in regions with orographic influences. The categorical analysis, including metrics like Probability of Detection (POD), False Alarm Ratios (FAR), and Critical Success Index (CSI), confirms GSMaP's stronger ability to detect light, moderate, and heavy rainfall events. Its better performance in detecting a range of rainfall intensities

makes it a preferred choice for hydrological applications like flood forecasting and water resource management.

However, GSMaP and IMERG both face limitations in detecting extreme rainfall events, particularly for very heavy rain (>124.5 mm). Although GSMaP performs better overall, both satellite products struggle with capturing the intensity of extreme weather, an area that needs improvement for more accurate flood forecasting and disaster preparedness in regions like the Ganga Basin. GSMaP's demonstrated strengths in this study imply that it could be a vital tool for real-time hydrological modeling and water management. Its superior performance in detecting rainfall variability, particularly in agricultural regions, suggests it could help mitigate risks and optimize water resource planning. Nonetheless, enhancements in extreme rainfall detection are necessary to ensure that it fully meets the needs of flood risk assessment and other critical hydrological applications.

Conclusions

The analysis of the IMERG and GSMaP products relative to the IMD data for the Ganga River Basin provides valuable insights into their accuracy and reliability in capturing monsoon rainfall dynamics. Overall, the study offers several takeaways such that GSMaP shows superior performance in representing the spatial distribution of monsoon rainfall, especially in regions with complex topography, like the northern high-altitude areas. Its lower bias, RRMSE, and RMAE values, combined with higher Pearson's Correlation Coefficient (R_p), make GSMaP more suitable for large-scale precipitation analysis.

In context of Comparison of Strengths and Limitations, IMERG performs better in detecting Light and Moderate Rain events, showing higher POD and CSI values. However, it struggles with capturing spatial variability, often overestimating rainfall in northern mountainous areas and underestimating it in southern plains, revealing region-specific limitations of its algorithm in handling topographical changes. Whereas in Heavy Rain and Very Heavy Rain Detections, both the datasets face challenges, as indicated by high False Alarm Ratios (FAR) and low Probability of Detection (POD) values. This highlights the need for further development of rainfall retrieval methods to reduce the overestimation of extreme rainfall. The results underscore the importance of using satellite-based precipitation products like GSMaP for hydrological modeling and climate studies, especially in complex terrain areas. GSMaP's ability to capture long-term spatial rainfall trends makes it a valuable tool for

researchers and policymakers.

Future studies should focus on improving the algorithms of both IMERG and GSMaP, particularly for detecting extreme rainfall. Integrating satellite data with ground-based observations will enhance accuracy. Further validation with reliable local datasets is essential to assess satellite-based rainfall estimates in different geographical regions. In summary, the comparative analysis highlights GSMaP as a reliable source for large-scale spatial rainfall patterns, while IMERG is better at detecting localized rain intensity. These findings clarify the strengths and limitations of both products, aiding in better rainfall monitoring and climate research across the Ganga Basin and similar regions.

References

- AghaKouchak, A., Nasrollahi, N., Habib, E., 2009. Accounting for uncertainties of the TRMM satellite estimates. *Remote sensing*, 1(3), 606-619. <https://doi.org/10.3390/rs1030606>
- Funk, C., Peterson, P., Landsfeld, M., Pedreros, D., Verdin, J., Shukla, S., ... & Michaelsen, J. (2015). The climate hazards infrared precipitation with stations—a new environmental record for monitoring extremes. *Scientific data*, 2(1), 1-21.
- Ghajarnia, N., Liaghat, A., Arasteh, P.D., (2015). Comparison and evaluation of high resolution precipitation estimation products in Urmia Basin-Iran. *Atmospheric Research*, 158, 50-65. <https://doi.org/10.1016/j.atmosres.2015.02.010>
- Huffman, G.J., Bolvin, D.T., Nelkin, E.J., Wolff, D.B., Adler, R.F., Gu, G., Hong, Y., Bowman, K.P., Stocker, E.F., (2007). The TRMM multisatellite precipitation analysis (TMPA): Quasi-global, multiyear, combined-sensor precipitation estimates at fine scales. *Journal of hydrometeorology*, 8(1), 38-55. <https://doi.org/10.1175/JHM560.1>
- Jeniffer, K., Su, Z., Woldai, T., Maathuis, B., (2010). Estimation of spatial–temporal rainfall distribution using remote sensing techniques: a case study of Makanya catchment, Tanzania. *International journal of applied earth observation and geoinformation*, 12, S90-S99. <https://doi.org/10.1016/j.jag.2009.10.003>
- Joyce, R. J., Janowiak, J. E., Arkin, P. A., & Xie, P. (2004). CMORPH: A method that produces global precipitation estimates from passive microwave and infrared data at high spatial and temporal resolution. *Journal of hydrometeorology*, 5(3), 487-503.
- Kubota, T., Aonashi, K., Ushio, T., Shige, S., Takayabu, Y. N., Kachi, M., and Oki, R. (2020). Global Satellite Mapping of Precipitation (GSMaP) products in the GPM era. *Satellite Precipitation Measurement: Volume 1*, 355-373.
- Kumar, P., Gairola, R., Kubota, T., and Kishtawal, C. (2021). Hybrid assimilation of satellite rainfall product with high density gauge network to improve daily estimation: A case of Karnataka, India. *Journal of the Meteorological Society of Japan. Ser. II*, 99(3), 741-763.
- Kumar, P., Varma, A. K., Kubota, T., Yamaji, M., Tashima, T., Mega, T., and Ushio, T.

(2022). Long-Term High-Resolution Gauge Adjusted Satellite Rainfall Product Over India. *Earth and Space Science*, 9(12), e2022EA002595.

Kumar, P., Srivastava, S.S., Jivani, N., Varma, A.K., Yokoyama, C. & Kubota, T. (2024). Long-term assessment of ERA5 reanalysis rainfall for lightning events over India observed by Tropical Rainfall Measurement Mission Lightning Imaging Sensor. *Quarterly Journal of the Royal Meteorological Society*, 150(761), 2472–2488. <https://doi.org/10.1002/qj.4719>

Mega, T., Ushio, T., Matsuda, T., Kubota, T., Kachi, M., and Oki, R. (2019) Gauge-Adjusted Global Satellite Mapping of Precipitation. *IEEE Transactions on Geoscience and Remote Sensing*, 57(4), 1928-1935.

Sharifi, E., Steinacker, R., Saghafian, B., (2016). Assessment of GPM-IMERG and other precipitation products against gauge data under different topographic and climatic conditions in Iran: Preliminary results. *Remote Sensing*, 8(2), 135. <https://doi.org/10.3390/rs8020135>

Annexure

List of Tables

Table 1: Continuous Evaluation Metrics used in the study.

Table 2: Categorization of precipitation events.

Table 3: Categorization of satellite rainfall intensities events.

Table 4: Categorical Evaluation Metrics used in the study.

List of Figures

Figure 1: Study area map

Figure 2: IMD JJAS Average

Figure 3: IMERG JJAS Average

Figure 4: GSMaP JJAS Average

Figure 5: Relative Bias (IMERG vs IMD)

Figure 6: Relative Bias (GSMaP vs IMD)

Figure 7: RRMSE (IMERG vs IMD)

Figure 8: RRMSE (IMERG vs IMD)

Figure 9: RMAE (IMERG vs IMD)

Figure 10: RMAE (GSMaP vs IMD)

Figure 11: CC (IMERG VS IMD)

Figure 12: CC (GSMaP VS IMD)

Figure 13: Probability of Detection (POD)

Figure 14: False Alarm ratio (FAR)

Figure 15: Critical Success Index (CSI)

Figure 16: Frequency Bias Index (FBI)